

BITLIS EREN ÜNIVERSITESI FEN BILIMLERI DERGISI

FEN BILIMLER DERGISI

ISSN: 2147-3129 / e-ISSN: 2147-3188

Article Type: Research Article Received : May 1, 2025 : July 9, 2025 Revised Accepted : August 1, 2025

DOI : 10.17798/bitlisfen.1688568 Year :2025 :14 Volume Issue :3

Pages : 1636-1654



COMPARATIVE PERFORMANCE ANALYSIS OF PERMANENT MAGNET AND CLAW-POLE ALTERNATORS IN INTERNAL COMBUSTION ENGINES

Metin KAYNAKLI 1,* (D), Ahmet ALBAYRAK 2 (D), Raif BAYIR 3 (D)

¹ Bitlis Eren University, Vocational School of Technical Sciences, Bitlis, Türkiye

² Düzce University, Computer Engineering Department, Düzce, Türkiye

³ Karabük University, Mechatronic Engineering, Karabük, Türkiye

* Corresponding Author: mkaynakli@beu.edu.tr

ABSTRACT

In this study, a comprehensive experimental comparison of Permanent Magnet Alternators (PMA) and Claw-Pole Alternators (CPA) used in internal combustion engines (ICE) was conducted under three different operating conditions: no-load, loaded, and charging scenarios. Key performance parameters including voltage, current, engine speed, temperature variation, and fuel consumption were measured and analyzed in detail using a custom-built test setup and data acquisition system. The results show that while PMAs provide higher efficiency and power output under load, they are prone to higher operating temperatures and efficiency losses under no-load and charging conditions compared to CPAs. CPAs, on the other hand, demonstrated stable performance and higher current generation capacity, which is crucial for meeting increasing electrical demands in modern vehicles. The findings underline the importance of predicting alternator performance for optimizing fuel economy, enhancing electrical system reliability, and supporting the development of next-generation automotive alternators. Design recommendations are also presented to improve the efficiency and thermal management of PMAs in practical applications.

Permanent magnet alternator (PMA), Claw-Pole alternator (CPA), Fuel **Keywords:** efficiency in alternators, Automotive electrical systems.

1 INTRODUCTION

Disposing of with the rapid advancement of modern automotive technology, key issues such as meeting the increasing energy demand with low power consumption, improving the efficiency of electrical systems, and achieving fuel savings have come to the forefront. These needs are driving research into alternative energy generation methods and encouraging the automotive industry to seek innovative solutions. The electrical systems in vehicles play a critical role in ensuring safety and comfort. These systems not only power various electrical loads such as headlights, turn signals, windshield wipers, and radios, but also ensure that the battery remains continuously charged. Insufficient performance or complete failure of the electrical system poses a significant risk that can directly compromise driving safety.

The battery, one of the fundamental components of the vehicle's charging system, cannot meet the entire electrical power demand due to its limited capacity. Therefore, an additional power generation system is required to ensure that the battery remains fully always charged. When the engine is off, electrical loads are powered directly by the battery; however, when the engine is running, this responsibility is taken over by the charging system. Nonetheless, when the engine is operating at low speeds, the current produced by the charging system may not be sufficient to power the electrical loads. In such cases, the alternator and the battery work together to supply power. Under high engine speed conditions, the alternator not only powers the electrical loads but also charges the battery [1], [2].

CPAs, which are widely used in modern vehicles, have long been favored by the automotive industry due to their low cost, durability, and ability to maintain consistent efficiency within certain speed ranges [3], [4]. However, the increasing number of electronic components in modern vehicles and the resulting rise in energy demand have led to the inadequacy of traditional alternators. Consequently, various technological innovations are being researched to enhance the output power, efficiency, and overall performance of alternators [5], [6].

Among the methods developed to improve alternator efficiency are the addition of harmonic suppression diodes, the use of permanent magnets, twin-rotor designs, and the precise control of output voltages using power electronics techniques [7], [8]. However, the need to ensure sufficient electrical generation even at low engine speeds has driven vehicle manufacturers to explore alternative system solutions. In this context, permanent magnet alternators (PMAs) have emerged as a new generation of alternators, attracting attention with their high efficiency, high power output, low moment of inertia, and simple structure [9].

Fuel economy is one of the key factors in alternator selection. In CPAs, more mechanical power is required to reach the targeted current levels, which directly increases the engine's fuel

consumption [10]. Since alternators are directly connected to the engine via a belt, this leads to additional fuel usage during the energy generation process. On the other hand, in PMAs, fuel consumption is reduced due to minimized mechanical losses, thereby providing an economic advantage [11], [12].

In a study conducted by Huang and colleagues, a claw-pole magnetic levitation torque motor (CPMLTM) was developed, and it was demonstrated that the motor could suspend the rotor in a neutral axial and circumferential position through cogging torque and axial restoring forces between the stator claw poles and the permanent magnets on the rotor [13].

Wu and his colleagues investigated the effects of stator tooth deformation on electromagnetic force harmonics and acoustic noise in claw-pole alternators. Their study showed that deformation, particularly when the number of rotor pole pairs is not an exact multiple, leads to the generation of additional spatial harmonic components [14]. Furthermore, the same researchers proposed a new rotor topology and demonstrated that electromagnetic noise in claw-pole alternators could be reduced. Simulation results revealed that by offsetting the N and S poles in the same direction, electromagnetic noise could be reduced by up to 6.7 dB(A) [15].

In this context, the importance of PMAs, which offer higher efficiency and lower mechanical losses, is increasing in vehicle applications. Existing studies in the literature highlight the advantages and potential application areas of PMAs compared to CPAs, but they also underscore certain technical limitations [16]–[19].

In a study conducted in 2024, a multi-phase configuration approach was tested in a simulation environment to provide high energy storage density and longer service life. Simulations and experimental results confirmed the effectiveness of the mathematical model, while the proposed phase-shifting fault-tolerant control technique increased the operational reliability of the system [37.]

A new cooling technique was developed to improve the thermal characteristics of a permanent magnet generator (PMG) by integrating it with an earth-air heat exchanger (EAHE). The results show that the maximum temperature reduction of the end winding of the PMG is 24.45% due to EAHE when the PMG operates at full load. In addition, the maximum temperature reduction of the end winding of the PMG is 50.91% due to EAHE when the PMG operates at variable load. The use of EAHE together with PMG resulted in an 8.06% reduction in annual total cost [38].

Therefore, detailed prediction of the performance of PMA and CPA is of great importance for the efficient and reliable operation of vehicle electrical systems under different engine speeds and variable load conditions. Predicting performance in advance allows the selection of the right alternator type, optimization of fuel consumption and increased system reliability. In addition, clearly demonstrating the advantages and limitations of both alternator types under real operating conditions provides important inputs for the design of next-generation alternators.

In this study, the performance of a CPA used in internal combustion engines, and a permanent magnet rotor alternator was experimentally compared under different operating conditions. The measured parameters included alternator voltage and current, load voltage and current, engine speed, temperature variations, and fuel consumption. Based on the findings, the strengths and weaknesses of both alternator types in terms of performance were evaluated, and recommendations were provided for potential automotive applications.

2 MATERIAL AND METHOD

2.1 Permanent Magnet Alternators

Today, CPAs are proving insufficient to meet the increasing electrical energy demands of vehicles. This has led alternator manufacturers to develop new solutions that provide higher power and efficiency output. Among the methods developed are approaches such as increasing the alternator's rotational speed, using power electronics technologies to make the generated electricity more efficient, and reducing energy losses in the system. Research is also being conducted on different electrical machines and hybrid systems that could replace traditional alternators. The efficiency and overall performance of existing alternators remain limited, especially at certain engine speeds, where they fail to generate sufficient voltage [20,21]. With the rise in electrical loads, the necessity of generating adequate electricity even at low engine speeds is driving vehicle manufacturers to search for alternative systems [2]. One such alternative is the use of PMAs in electricity generation [5], [6].

Permanent magnets are materials that can generate a continuous magnetic field without the need for an external excitation current. They are typically made from alloys of elements such as iron, nickel, and cobalt, and have a high permanent flux density and high coercive force. These properties allow permanent magnets to create a strong magnetic field in the air gap of magnetic circuits. One of the most advanced types of permanent magnets today is the

Neodymium-Iron-Boron (NdFeB) magnet [22-24]. This magnet ranks among the materials with the highest energy density in commercial use. The key characteristics expected of an ideal permanent magnet include high internal coercive force, high saturation magnetization, high permanent flux density, and high energy density.

PMAs offer significant advantages due to their high efficiency, high power output, low moment of inertia, and simple structure. However, these systems also have some disadvantages. One major technical limitation is the difficulty in voltage regulation, particularly because the output voltage is sensitive to load variations and rotational speed. In automotive applications, this issue is one of the main barriers to the widespread adoption of PMAs [25,26]. However, since existing regulation systems can reduce high output voltages to 14V levels, this technology may also provide an advantage for PMAs. Furthermore, studies in the literature propose various mechanical solutions to control the magnetic flux generated in stator windings [39].

The output power of alternators varies depending on the engine's rotational speed. When the back electromotive force (EMF) voltage exceeds the output voltage, the alternator reaches its maximum power. Although the back EMF voltage in PMAs can reach around 80V, the system must maintain a constant output voltage of 14V, so the desired current can only be achieved at higher speeds. Additionally, the leakage reactance of the rotor limits the alternator's output power capacity [27-29]. While operating under load, the voltage drop across this leakage reactance becomes noticeable, and this drop increases with both rotational speed and the drawn current. As a result, when high current is drawn, a noticeable decrease in alternator output voltage occurs [4].

In permanent magnet alternators, most losses at low and medium engine speeds are due to stator copper losses. Iron losses, on the other hand, become dominant only at high speeds. The overall efficiency of these types of alternators typically ranges from 60% to 80%, and this efficiency range is usually achieved between 500 and 2000 revolutions per minute (rpm) [2].

2.2 Design Characteristics of the PMA

PMAs are preferred for their ability to provide high power and efficiency. Their ease of manufacturing and compact structure make them well-suited for vehicle applications, increasing their usability in the automotive industry [30]. Magnetic flux density is a key parameter in electricity generation; thanks to the high flux density of the permanent magnets used, the overall size of the alternator can be reduced. PMAs consist of a structure that includes

permanent magnets mounted on the rotor and three-phase stator windings. A direct current (DC) voltage is obtained at the alternator output via a full-wave rectifier circuit.

PMAs offer attractive solutions, particularly in renewable energy systems, due to their high conversion efficiency. In addition, their lack of need for external excitation current and the absence of brushes or slip rings result in significantly reduced mechanical friction. Their simple and compact design also provides major advantages in terms of durability and reliability. However, these systems do have certain disadvantages. One of the most significant limitations is the high cost of the permanent magnets that enable such high efficiency. As efficiency increases, so does the cost of the magnets [31].

Another major disadvantage of this type of alternator is that the output voltage varies directly with the rotor speed. This poses a significant regulation problem for applications requiring a constant output voltage and represents a technical challenge that must be addressed. The main losses affecting the performance of PMAs include mechanical friction, magnetic losses, stator copper losses, and rectifier-related losses. To analyze these losses and to model the overall operating characteristics of the alternator, an equivalent circuit of the system has been developed. Figure 1 shows the equivalent circuit of the PMA. This equivalent circuit enables the simulation of both the mechanical and electrical variables of the PMA [32].

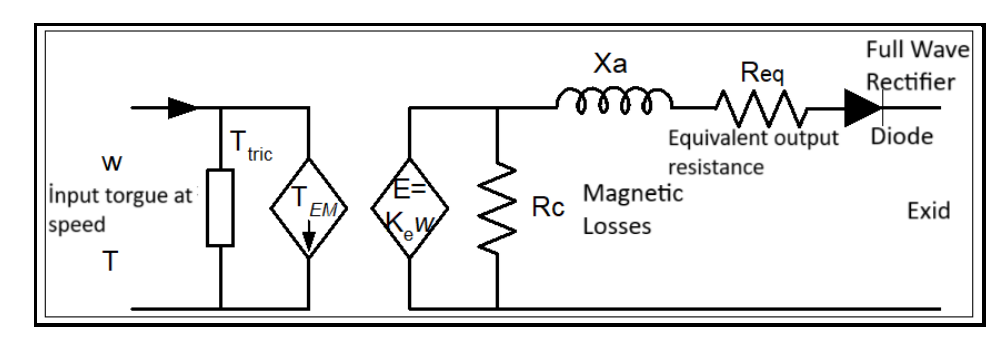


Figure 1. Equivalent circuit of the PMA

In PMAs, although there are no losses caused by brushes, there are still losses resulting from bearings. Bearings are found in all electric machines, and the losses arising from them include:

$$P_{fric} = T_{fric} \cdot \omega \tag{1}$$

Equation (1) dE Tfric is the friction torque. This torque can be measured at low speeds. However, friction losses due to the existing cooling fan inside the machine can be neglected. Eddy currents and hysteresis losses in magnetic materials are magnetic losses. These losses vary according to the axial flux fatigue and can be calculated by the formula in equation (2).

$$P_e + P_h = K_e \cdot f^2 \cdot B_{max}^2 + K_h \cdot f \cdot B_{mav}^{\chi} \tag{2}$$

The constant x in the equation is a constant value ranging from 1.5-2.5. Great care should be taken in measuring the losses in a permanent magnet machine operating without load. Because magnetic losses vary proportional to the square of the inverse EMC. Total magnetic losses can be expressed in equation (3).

$$P_e + P_h = K_e \cdot f^2 \cdot B_{max}^2 + K_h \cdot f \cdot B_{mav}^x \tag{3}$$

$$P_e P_m = K_m \cdot \omega^2 \tag{4}$$

$$P_e P_{Cu} = I_{dc}^2 \cdot R_{eq} \tag{5}$$

Copper losses can be expressed in equation (4) as resistance dependent losses. Rectifier losses are the voltages dropping across the full wave rectified diodes. This is given in equation (5).

2.3 Design Characteristics of The Pma

To test the performance of the alternator in real time on an ICE, a custom experimental setup was developed. This setup includes mechanical and electronic connections between the alternator integrated into the ICE and a computer system used for data acquisition and analysis. The block diagram of the experimental setup is presented in Figure 2(a). The general layout of the engine and system components used in the experimental setup is shown in Figure 2.(b). The experimental setup consists of a test stand with upper and lower chassis, Fiat brand 1.6L spark ignition engine, various electrical receivers (headlight and rear lighting systems, side and rear signal systems, windshield wiper motor and power window lifting systems), precision fuel measuring cup and amplifier, thermocouple sensor and amplifier for temperature measurements, magnetic sensor and amplifier for speed measurements, current and voltage measurement devices, PCLD-8710 terminal tube, PCL-1716L data exchange card and a desktop computer. The claw type alternator used in the experiments was manufactured by MAKO and is a model with the technical specifications of 12V AA125R-14V-45A, which is widely available on the market.

(b)

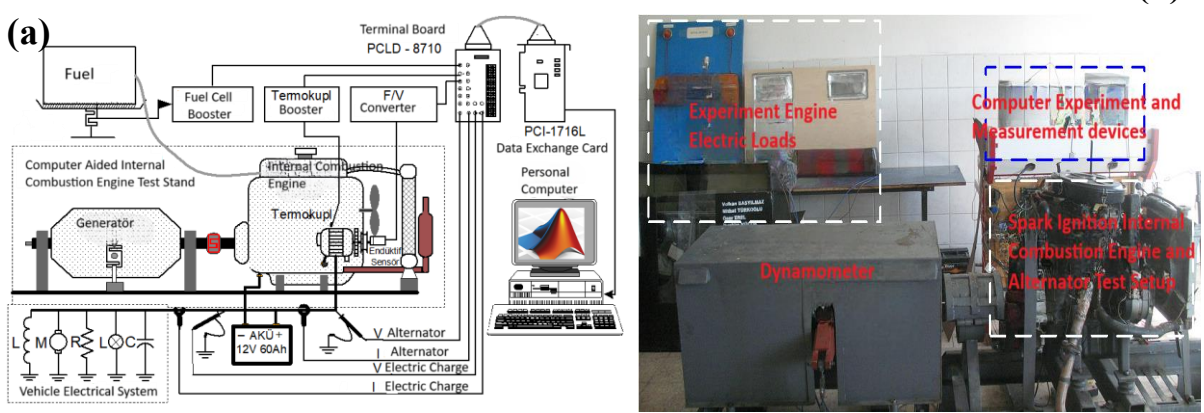


Figure 2. (a) Block diagram of the experimental setup; (b) general view of the experimental setup.

Another alternator used in the experimental setup is a two-phase PMA manufactured by Efor Endüstriyel Tasarım Sanayi Ticaret. Figure 3(a) shows the CPA, while Figure 3(b) illustrates the PMA.

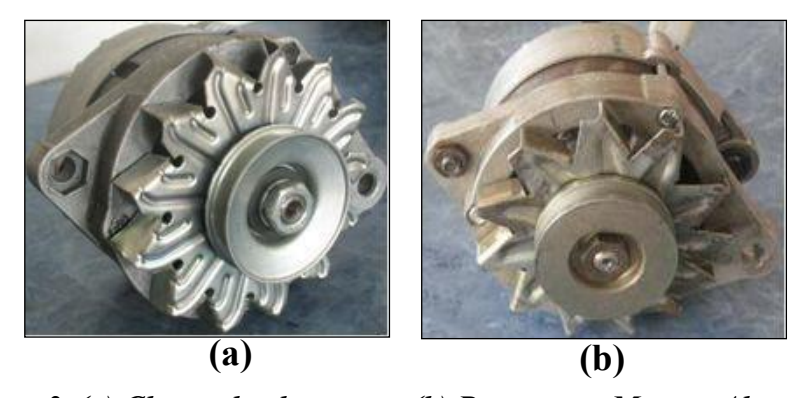


Figure 3. (a) Claw pole alternator; (b) Permanent Magnet Alternator.

In the experiments, three different performance measurement conditions were applied to both the CPA and the PMA. These conditions were as follows: no-load performance measurements, loaded performance measurements, and charging performance measurements.

In the no-load performance tests carried out in the first phase, the ICE was operated at a constant 2000-2100 rpm range and the alternators were allowed to operate at 4000-4200 rpm for one hour without any electrical load being connected to the circuit. In these tests, the power generated by the alternators, the amount of power drawn from the battery by the electrical loads in the system, the temperature changes during operation and the effects of the alternators on the fuel consumption of the engine were measured. The measurements were recorded in real time on a model created in MATLAB environment with the help of precision measuring devices and a data exchange card. In the second stage, during the loaded performance tests, the no-load experimental conditions were maintained. However, this time, during the alternator operation,

specific electrical loads (fan, headlights, signals, wiper motors, and resistors) were sequentially activated in ten-minute intervals. In these tests, the changes in the parameters measured during the no-load condition under load were analyzed. This allowed for the evaluation of the alternators' performance characteristics under load conditions. In the third and final experimental stage, charging performance tests were conducted. In these tests, the operating conditions from the no-load and loaded tests were maintained [33]. However, without activating any electrical loads, a fully discharged battery was charged under a fixed engine speed using the alternator. During this process, the changes in the parameters measured in the previous tests during the charging process were observed and a comparative analysis was performed.

3 PERFORMANCE MEASUREMENTS OF CPA AND PMA

3.1 No-Load Performance Measurements of CPA

In Figure 4 (a), the power-time graph obtained by multiplying the instantaneous voltage and current values produced during one hour of operation at a constant 4000–4200 rpm range of the CPA is presented.

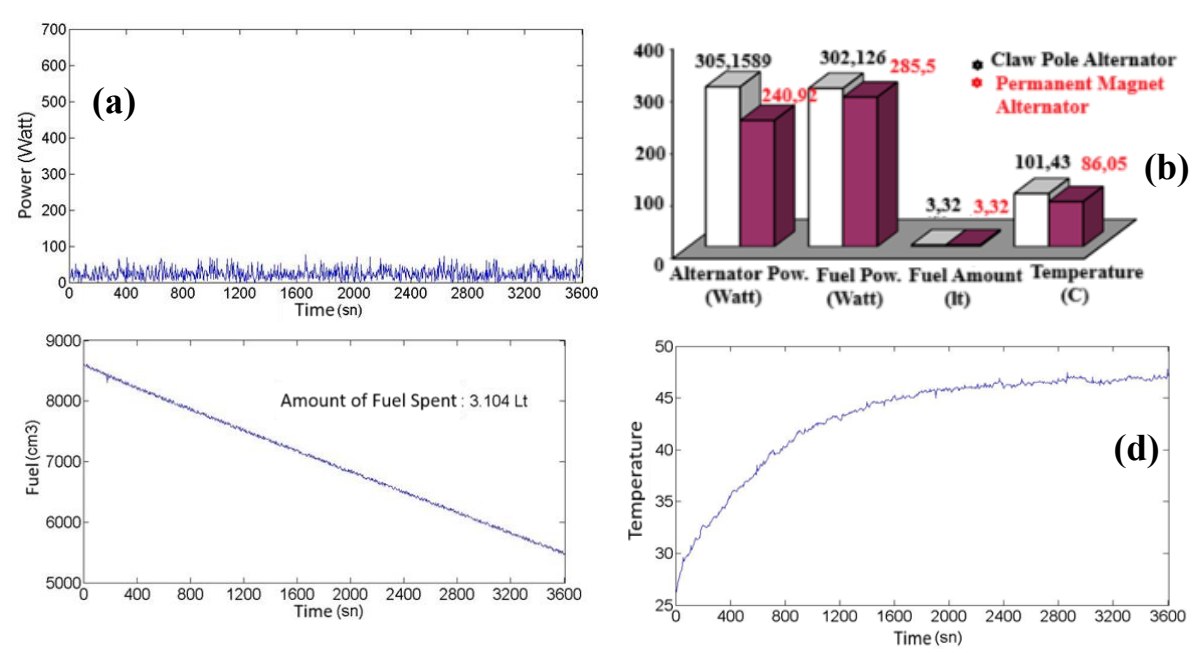


Figure 4. (a) Alternator power graph; (b) load power graph; (c) fuel consumption graph; (d) alternator temperature graph.

In Figure 4 (b), the load power (theoretical power that electrical consumers could draw) is shown, which is obtained by multiplying the measured voltage and current values across the battery when no electrical load is connected to the circuit, at a constant engine and alternator

speed. Figure 4 (c) shows the amount of fuel consumed per unit time by the internal combustion engine during the operation of the alternator, illustrating the fuel performance of the engine in interaction with the alternator. Finally, Figure 4 (d) displays the temperature change over time measured on the alternator body during the no-load operation of the CPA.

3.2 Loaded Performance Measurements of CPA

In Figure 5 (a), the power-time graph obtained for the case when the CPA operates under load is presented. In this experiment, no electrical load was connected to the system during the first 10 minutes; then, electrical consumers were gradually connected at 10-minute intervals. This allowed for the evaluation of the power performance produced by the CPA at different load levels over time. In Figure 5 (b), during the fixed engine and alternator speed, the time-dependent variation in the power drawn from the battery is shown as electrical loads are activated while the alternator powers the battery.

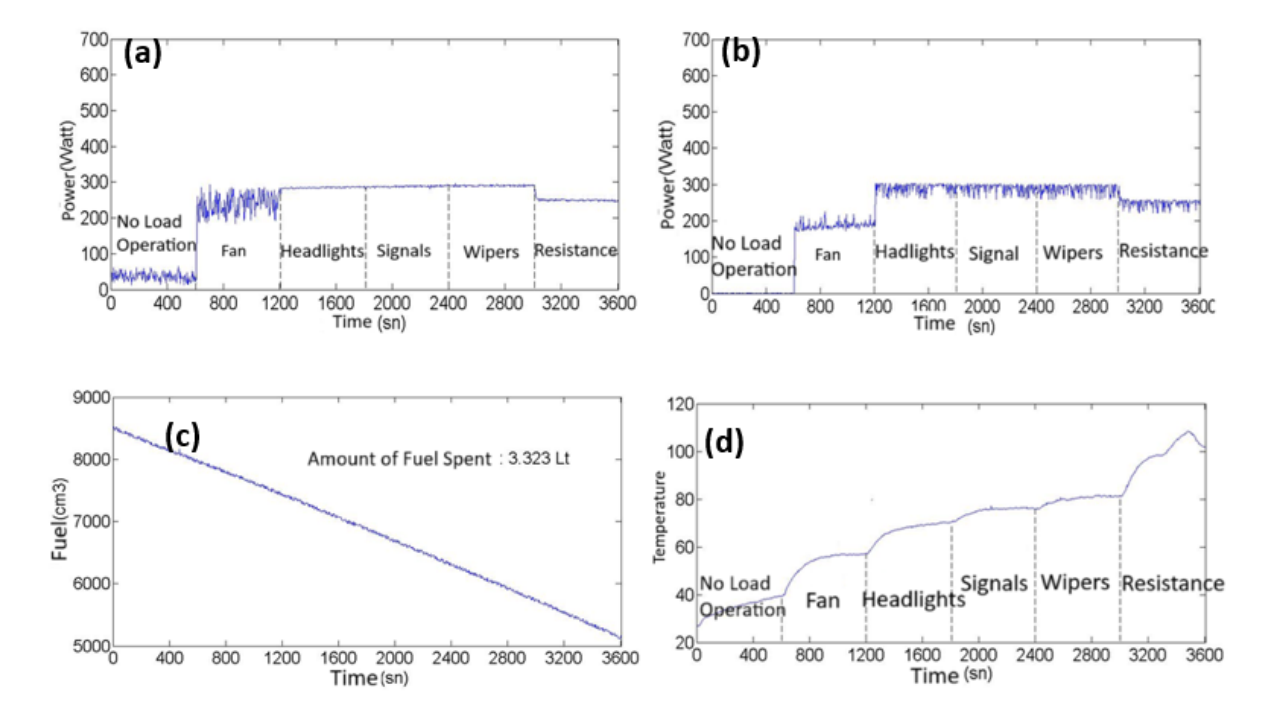


Figure 5. (a) Alternator power graph; (b) load power graph; (c) fuel consumption graph; (d) alternator temperature graph.

Figure 5 (c) illustrates the amount of fuel consumed per unit time by the internal combustion engine under load conditions of the CPA, revealing the impact of the electrical load on the engine. Finally, in Figure 5 (d), the temperature-time change graph for the CPA operating under load at a fixed engine and alternator speed is presented, monitoring the thermal behavior of the alternator.

3.3 Performance Measurements of CPA during Charging

In Figure 6 (a), the graph showing the time-dependent variation of the electrical power produced by the CPA during battery charging is presented. This graph reveals the dynamic changes in the alternator's power output throughout the charging process. In Figure 6 (b), under fixed engine and alternator speed, the time-dependent change in the amount of power drawn by electrical consumers from the battery during the charging process is provided. Figure 6 (c) shows the amount of fuel consumed by the internal combustion engine when the alternator is only charging the battery, allowing for the evaluation of the impact of the charging load on the engine. Finally, in Figure 6 (d), the time-dependent graph of the temperature changes in the structure of the CPA during the battery charging process is presented, contributing to the thermal behavior analysis.

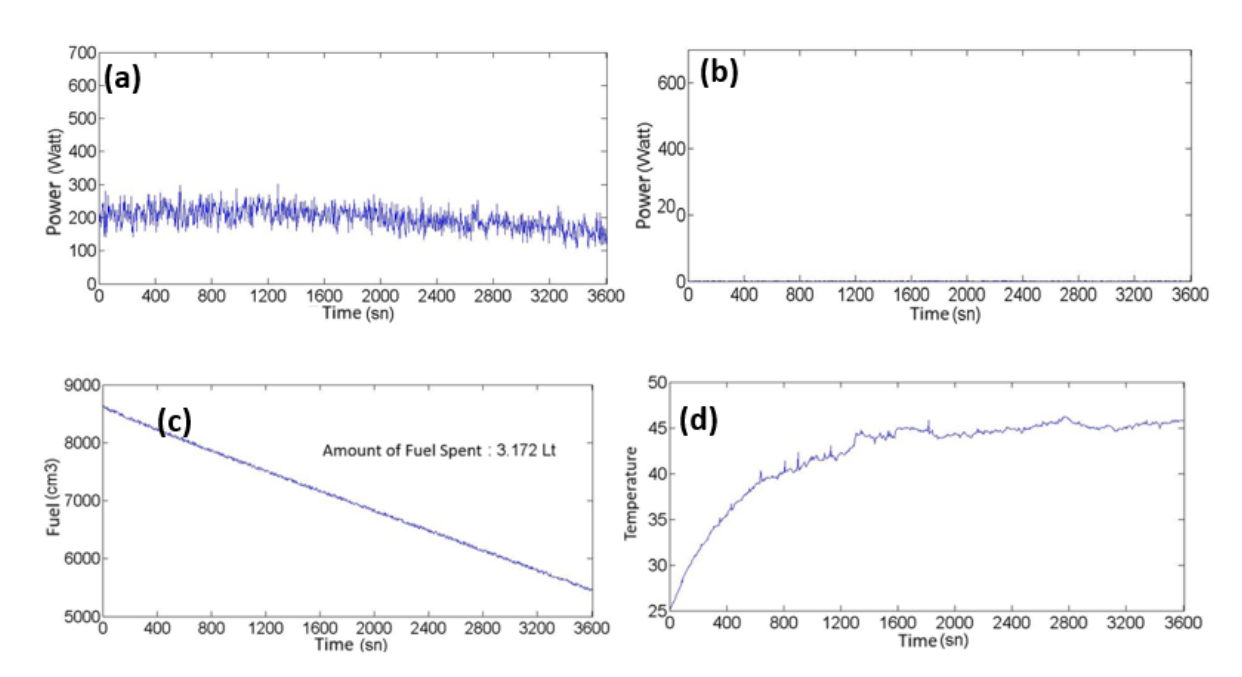


Figure 6. (a) Alternator power graph; (b) load power graph; (c) fuel consumption graph; (d) alternator temperature graph.

3.4 No-Loaded performance measurements of the PMA.

In this experimental phase, the conditions applied during the no-load performance tests of the CPA were identically applied to the PMA to measure its performance values under similar conditions. Figure 7 (a) presents the power-time graph showing the time-dependent variation of the power output produced by the PMA during one hour of operation at a constant speed range of 4000–4200 rpm. In Figure 7 (b), under fixed engine and alternator speed, the time-dependent variation of the load power—calculated by multiplying the voltage and current values measured across the battery without connecting any electrical load to the system—is

shown. This graph represents the potential power supplied to the battery by the PMA under no-load conditions. Figure 7 (c) shows the amount of fuel consumed per unit time by the internal combustion engine due to the mechanical load applied by the PMA operating at constant speed. Finally, Figure 7 (d) presents the time-dependent graph of temperature changes observed on the alternator body during the PMA's no-load operation at constant engine speed [34].

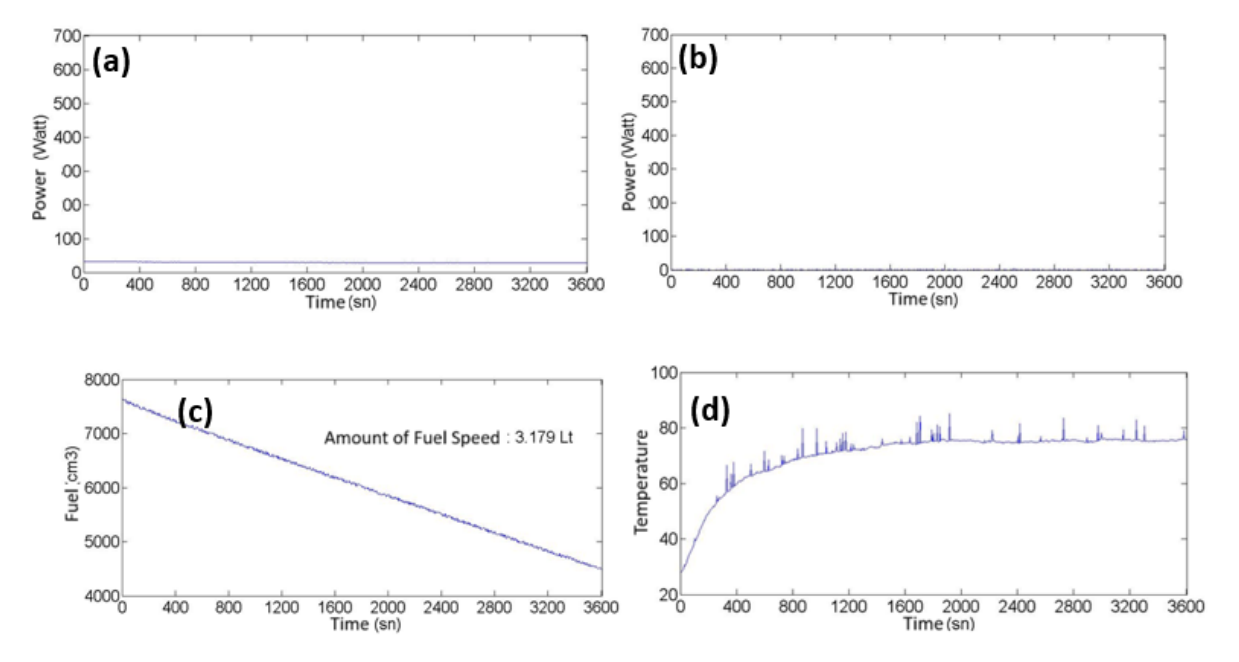


Figure 7. (a) Alternator power graph; (b) load power graph; (c) fuel consumption graph; (d) alternator temperature graph.

3.5 No-Loaded performance measurement graphs of the PMA

In this experiment, the loaded performance test conditions applied to the CPA were similarly applied to the PMA, and the performance values of the PMA were measured under comparable conditions. Figure 8 (a) presents the power-time graph showing the time-dependent variation in the power generated by the PMA under conditions where electrical loads were sequentially activated. In Figure 8 (b), under constant engine and alternator speed, the time-dependent variation of the power drawn from the battery by these electrical loads as they were connected one by one is shown. Figure 8 (c) illustrates the change in the amount of fuel consumed per unit time by the internal combustion engine during the PMA's operation under load. Finally, Figure 8 (d) shows the temperature-time graph reflecting how the temperature on the alternator body changed over time while the PMA operated under load conditions.

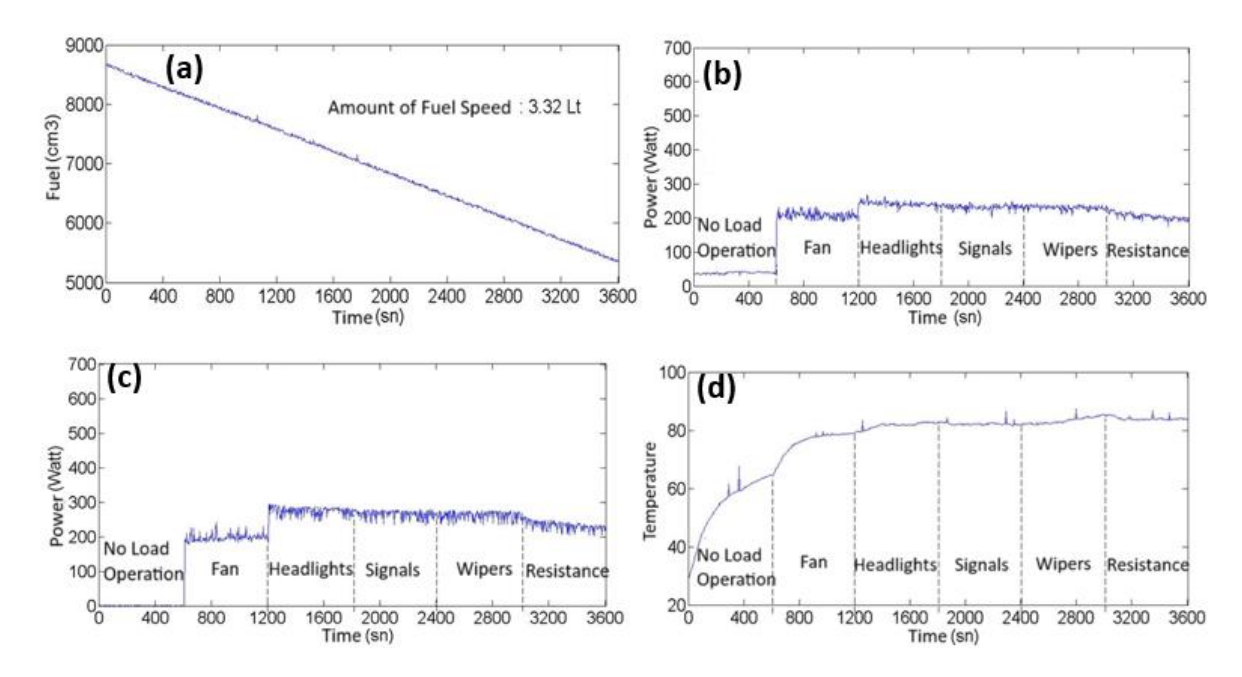


Figure 8. (a) Alternator power graph; (b) load power graph; (c) fuel consumption graph; (d) alternator temperature graph.

3.6 Loaded Performance Measurements of The PMA

Figure 9 (a) presents the power-time graph showing the time-dependent variation of the power output generated by the PMA during the charging process. This graph reflects the power performance of the alternator under conditions where it is solely charging an empty battery. In Figure 9 (b), under constant engine and alternator speed, the load power-time graph shows the time-dependent variation of the power drawn from the battery by electrical consumers as they are activated during the charging process. Figure 9 (c) illustrates the change in the amount of fuel consumed per unit time by the internal combustion engine during the operation of the PMA while charging. Finally, Figure 9 (d) presents the temperature-time graph that monitors the rise in temperature on the alternator body over time during the battery charging process carried out solely by the PMA.

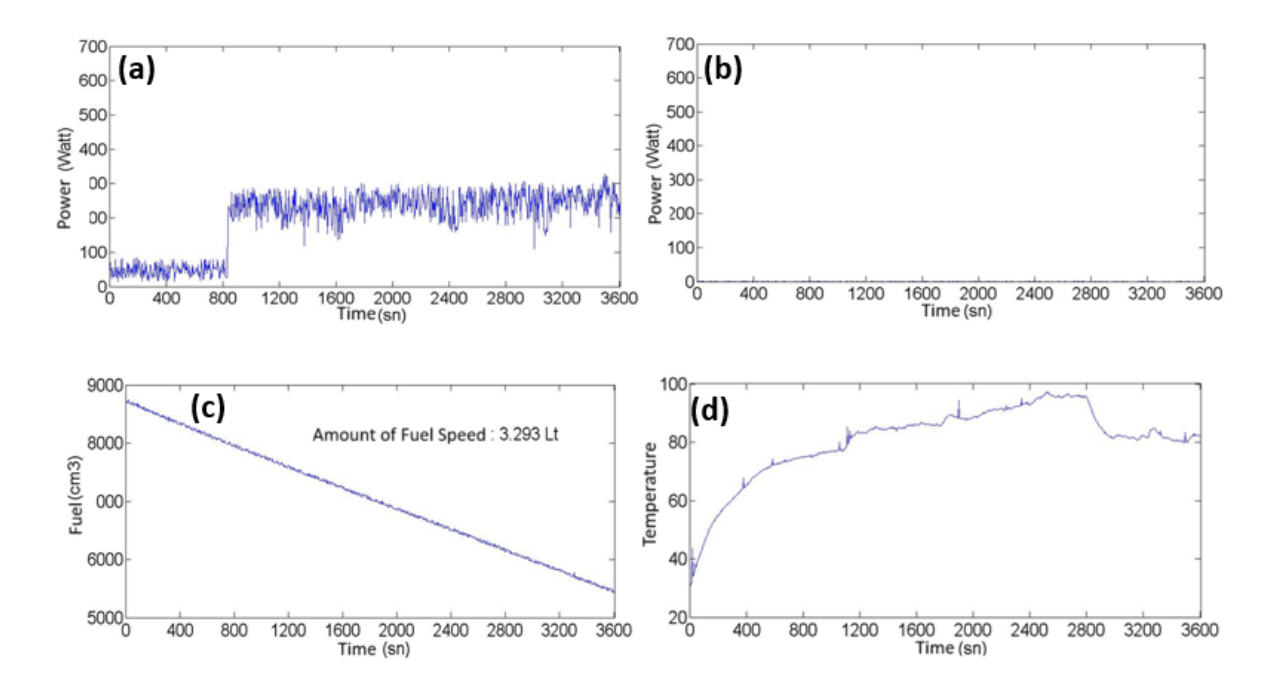


Figure 9. (a) Alternator power graph; (b) load power graph; (c) fuel consumption graph; (d) alternator temperature graph.

The graphical comparison of the measurement data obtained under no-load experimental conditions for both the CPA and PMA is presented in Figure 10. According to the findings, the CPA demonstrated higher performance compared to the PMA in terms of both alternator output power and power drawn by the load. On the other hand, when temperature measurements were evaluated, it was observed that the PMA heated up more than the CPA during operation. This suggests that the PMA may pose a potential disadvantage in terms of thermal durability and component life during prolonged use. The impact of both alternators on the fuel consumption of the internal combustion engine was similar, and no significant difference was observed.

The graphical comparison of the measurement data obtained under loaded experimental conditions for both the CPA and PMA is presented in Figure 12. According to the experimental results, it was observed that the amount of power produced by the PMA was lower compared to the CPA. However, since no electrical loads were connected to the system during the experiment, the power drawn by the load remained at 0 watts for both alternators. In terms of fuel consumption, it was determined that the amount of fuel consumed per unit time by the internal combustion engine was similar for both alternators. Temperature measurements, under these experimental conditions, show that the PMA reached lower temperature values compared to the CPA, indicating that the PMA is thermally more advantageous [35].

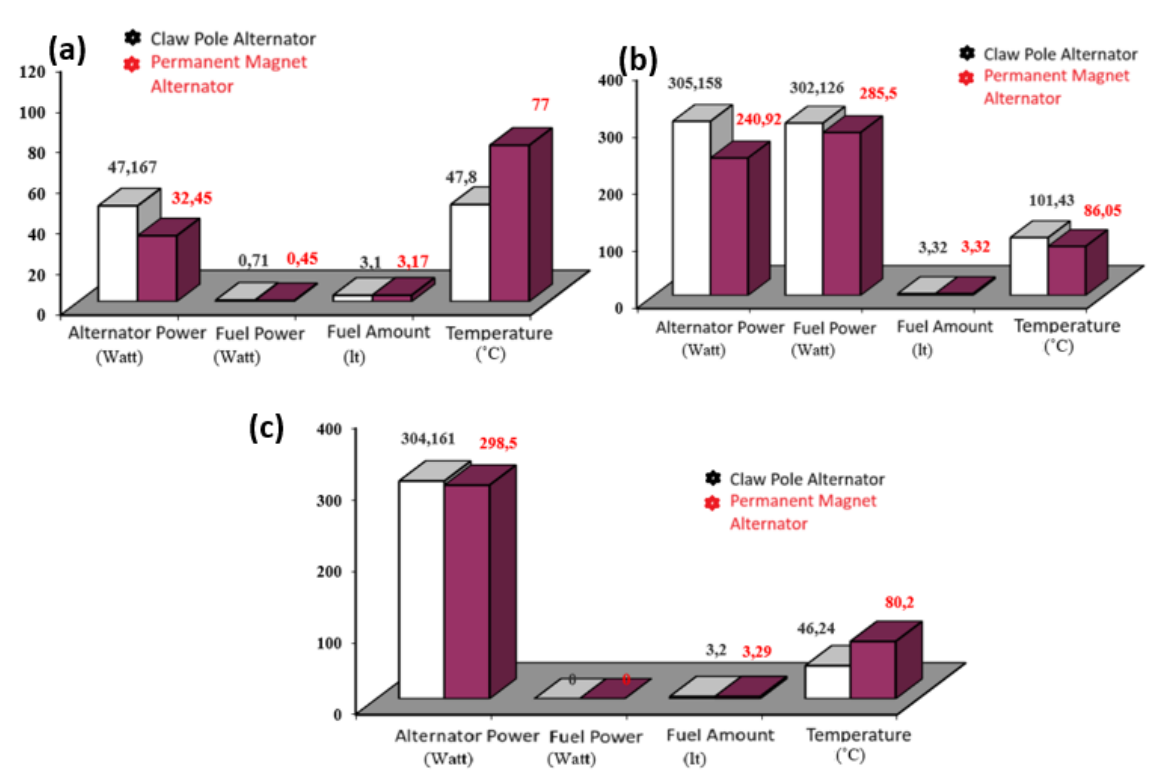


Figure 10. (a) No-load performance measurement graphs; (b) loaded performance measurement graphs; (c) charging performance measurement graphs.

The comparative graphical presentation of the experimental measurement data obtained during the charging process is provided in Figure 13. The analysis conducted at this stage revealed that the power level produced by the PMA is quite like that of the CPA. However, since electrical loads were not actively connected to the system during these tests as well, the load power values were again measured at 0 watts. In terms of fuel consumption, it was determined that the impact of both alternators on the internal combustion engine was similar. On the other hand, when temperature values were examined, it was found that the PMA reached higher temperatures compared to the CPA, indicating that this may be an unfavourable indicator of thermal performance for the PMA.

When the results obtained are examined in detail, it is seen that the high voltage values provided by PMA at high speeds are balanced by the limited current production capacity at low speeds compared to CPA. In the tests performed under load, CPA's current production provides an advantage, while PMA's low mechanical losses and lower temperature increase provide advantages in terms of thermal efficiency, especially in long-term use. In charging conditions, both alternator types showed similar performance, but it was determined that PMA reached higher temperature values. These results show that both alternators have advantages and disadvantages according to different operating conditions, and these data constitute an important reference in design developments [36].

4 RESULTS AND DISCUSSION

In this study, the CPA and the PMA were tested for one hour each under three different experimental conditions (no-load, loaded, and charging). During the experiments, the efficiencies of both alternators, their power generation performances, and their effects on the fuel consumption of the ICE were analyzed. The findings can be summarized as follows:

- As a result of the no-load experiments, it was determined that the PMA produced higher voltage values compared to the CPA in terms of both alternator and load voltage. However, in terms of current generation capacity, it was found that PMA fell short compared to CPA, and this was considered a negative performance indicator for the PMA. Additionally, considering the fuel consumption of the ICE and the temperatures reached by the alternators during operation, it was determined that the CPA was more advantageous than the PMA under these experimental conditions.
- In the loaded experiments, it was observed that the current production of the CPA was higher than the amount of current produced by the PMA. On the other hand, when evaluating other performance criteria such as alternator voltage, load voltage, load current, and temperature increase, it was determined that the PMA provided better results compared to the CPA. Under these experimental conditions, the effects of both alternators on the fuel consumption of the ICE were found to be very similar.
- In the charging experiments, it was recorded that the current values produced by the CPA were higher than those produced by the PMA. However, in terms of alternator voltage, load voltage, and load current, the PMA performed better compared to the CPA. Nevertheless, in this experiment as well, it was concluded that the PTA was more advantageous than the PMA in terms of temperature increase and fuel consumption.

As a result of the general evaluation, various design improvements have been proposed to enhance the performance of the PMA. Specifically, increasing the number of phases in the PMA, strengthening the stator windings, and using larger diameter and higher energy density permanent magnets in the rotor could significantly improve the efficiency of the alternator. Additionally, to prevent the temperature increase observed in the PMA, it is recommended to design these alternators with air- or water-cooling systems. With these improvements, it is expected that the performance of the PMA could surpass that of the CPA.

This study has some limitations. Experimental measurements were performed only on a specific internal combustion engine type and at specific speed ranges; similar performance results may not be obtained under different engine types, speed ranges or climatic conditions. In addition, the analysis method used is based on recording experimental data over time and processing it in MATLAB; this approach is limited in terms of validation and is planned to be supported by further modeling, long-term tests and different test scenarios. In future studies, it is aimed to expand the scope of the tests with different engine types and alternator configurations.

Conflict of Interest Statement

There is no conflict of interest between the authors.

Statement of Research and Publication Ethics

The study is complied with research and publication ethics.

Artificial Intelligence (AI) Contribution Statement

This manuscript was entirely written, edited, analyzed, and prepared without the assistance of any artificial intelligence (AI) tools. All content, including text, data analysis, and figures, was solely generated by the authors.

Contributions of the Authors

M.K. took part in the conduct of experimental studies, data collection, data analysis, and manuscript writing. A.A. took part in data collection, data analysis, and manuscript writing. R.B. contributed to the design of experimental studies, providing methodology and consulting services.

REFERENCES

- [1] D. J. Perreault and V. Caliskan, "Automotive power generation and control," *IEEE Trans. Power Electron.*, vol. 19, no. 3, 2004, doi: 10.1109/TPEL.2004.826432.
- [2] M. Naidu, "A high-efficiency high-power-generation system for automobiles," *IEEE Trans. Ind. Appl.*, vol. 33, no. 6, 1997, doi: 10.1109/28.649966.
- [3] W. Cai, "Comparison and review of electric machines for integrated starter alternator applications," in *Conf. Rec. IAS Annu. Meeting (IEEE Ind. Appl. Soc.)*, 2004. doi: 10.1109/ias.2004.1348437.
- [4] K. G. Bürger, "Alternators," in *Automotive Electric/Electronic Systems*, 2nd ed., A. Beer and A. Cypra, Eds., Stuttgart, Germany: Robert Bosch GmbH, 1995, pp. 304–345.
- [5] B. Singh, B. P. Singh, and S. Dwivedi, "A state of art on different configurations of permanent magnet brushless machines," *J. Inst. Eng. Electr. Eng. Div.*, vol. 87, no. JUNE, 2006.

- [6] R. Dutta and M. F. Rahman, "Design and analysis of an interior permanent magnet (IPM) machine with very wide constant power operation range," *IEEE Trans. Energy Convers.*, vol. 23, no. 1, 2008, doi: 10.1109/TEC.2007.905061.
- [7] J. Huang, Z. Song, S. Li, and J. Ruan, "Claw-pole magnetic levitation torque motor for 2D valve with automatic neutral adjustment," *IET Electr. Power Appl.*, vol. 17, no. 10, 2023, doi: 10.1049/elp2.12342.
- [8] S. Wu et al., "Influence of stator teeth deformation on the electromagnetic force and acoustic noise of claw pole alternators," *Electr. Eng.*, vol. 105, no. 5, 2023, doi: 10.1007/s00202-023-01919-y.
- [9] S. Wu, X. Yan, Z. Chen, Y. Zhang, and X. Feng, "New rotor topologies for electromagnetic forces and acoustic noise reduction of claw pole alternators," *J. Electr. Eng. Technol.*, vol. 18, no. 5, 2023, doi: 10.1007/s42835-023-01559-z.
- [10] F. R. Ismagilov, V. E. Vavilov, O. A. Yushkova, E. A. Pronin, and A. A. Zherebtsov, "Characteristics of the starter–alternator with incorporated permanent magnets made of a dual-phase magnetic material rotor," *J. Mach. Manuf. Reliab.*, vol. 52, no. 8, 2023, doi: 10.1134/S1052618823080071.
- [11] Safdar, S. Sultan, H. A. Raza, M. Umer, and M. Ali, "Empirical analysis of turbine and generator efficiency of a pico hydro system," *Sustain. Energy Technol. Assessments*, vol. 37, 2020, doi: 10.1016/j.seta.2019.100605.
- [12] N. Pamuk, "Investigation of interior permanent magnet synchronous (IPMS) machine applications in electrical vehicle engine industry," *TEM J.*, vol. 12, no. 4, 2023, doi: 10.18421/TEM124-04.
- [13] C. H. Cheng and S. Dhanasekaran, "Design of a slot-spaced permanent magnet linear alternator based on numerical analysis," *Energies*, vol. 15, no. 13, 2022, doi: 10.3390/en15134523.
- [14] C. H. Cheng and S. Dhanasekaran, "Cogging force reduction and profile smoothening methods for a slot-spaced permanent magnet linear alternator," *Energies*, vol. 16, no. 15, 2023, doi: 10.3390/en16155827.
- [15] S. Wu, S. Wu, J. Zhou, S. Cui, and X. Zhang, "Permanent magnet compensated pulsed alternator for driving air-based loads," *IEEE Trans. Transp. Electrif.*, vol. 6, no. 4, 2020, doi: 10.1109/TTE.2020.2988181.
- [16] O. Otuoze et al., "Field loss calculation of a wind-powered axial flux alternator by analytical equations," *Eng. Reports*, vol. 3, no. 9, 2021, doi: 10.1002/eng2.12391.
- [17] Y. Wan, Q. Li, J. Guo, and S. Cui, "Thermal analysis of a Gramme-ring-winding high-speed permanent-magnet motor for pulsed alternator using CFD," *IET Electr. Power Appl.*, vol. 14, no. 11, 2020, doi: 10.1049/iet-epa.2020.0086.
- [18] J. Cekani, F. G. Capponi, G. De Donato, and F. Caricchi, "Mechanical flux weakening methods for the achievement of a very wide constant power speed range in automotive applications," *IEEE J. Emerg. Sel. Top. Power Electron.*, vol. 10, no. 3, 2022, doi: 10.1109/JESTPE.2021.3058198.
- [19] Y. Cheng, G. Guo, and S. Hu, "Design and performance research of a novel iron-core permanent magnet compensated pulsed alternator with segmental squirrel-cage," *IEEE Trans. Ind. Electron.*, vol. 71, no. 2, 2024, doi: 10.1109/TIE.2023.3253922.
- [20] B. Thangaraj and R. Subramanian, "A comparative 3-D transient electromagnetic, thermal and powertrain study of single rotor BLPMSM and dual rotor machine for electric propelled vehicle," *Electr. Eng.*, vol. 103, no. 6, 2021, doi: 10.1007/s00202-021-01257-x.
- [21] S. Kirubadevi and S. Sutha, "PMSG based wind energy conversion system using intelligent MPPT with HGRSC converter," *Intell. Autom. Soft Comput.*, vol. 34, no. 2, 2022, doi: 10.32604/iasc.2022.025395.
- [22] H. Moradi CheshmehBeigi, "Slotless tubular PM generator with dual quasi-Halbach magnetized PM array: Analytical and numerical magnetic field analysis," *Int. J. Numer. Model. Electron. Networks, Devices Fields*, vol. 33, no. 2, 2020, doi: 10.1002/jnm.2569.
- [23] D. Karaoglan, D. G. Ocaktan, A. Oral, and D. Perin, "Design optimization of magnetic flux distribution for PMG by using response surface methodology," *IEEE Trans. Magn.*, vol. 56, no. 6, 2020, doi: 10.1109/TMAG.2020.2986187.
- [24] R. B. Godoy, M. A. G. de Brito, R. C. Garcia, M. L. M. Kimpara, and J. O. P. Pinto, "Integrated starter alternator PMSM drive for hybrid vehicles," *J. Control. Autom. Electr. Syst.*, vol. 32, no. 1, 2021, doi: 10.1007/s40313-020-00665-x.

- [25] M. C. Kulan, N. J. Baker, and S. Turvey, "Manufacturing challenges of a modular transverse flux alternator for aerospace," *Energies*, vol. 13, no. 6, 2020, doi: 10.3390/en13164275.
- [26] G. Vijayasree, V. P. Mini, and S. UshaKumari, "Investigation of magnetic effect in high-speed homopolar inductor alternator," *J. Electr. Eng. Technol.*, vol. 19, no. 5, 2024, doi: 10.1007/s42835-023-01774-8.
- [27] M. Murshed, M. Chamana, K. E. K. Schmitt, R. Bhatta, O. Adeyanju, and S. Bayne, "Design and performance analysis of a grid-connected distributed wind turbine," *Energies*, vol. 16, no. 15, 2023, doi: 10.3390/en16155778.
- [28] M. C. Kulan, N. J. Baker, and S. Turvey, "Impact of manufacturing and material uncertainties in performance of a transverse flux machine for aerospace," *Energies*, vol. 15, no. 20, 2022, doi: 10.3390/en15207607.
- [29] L. Jing, G. Liu, X. Guo, and S. Su, "Research on the cloud computing fuzzy proportion integration differentiation control strategy for permanent-magnet homopolar motor with salient pole solid rotor used on new-energy vehicle," *Sustain. Energy Technol. Assessments*, vol. 52, 2022, doi: 10.1016/j.seta.2022.101969.
- [30] R. Mirzahosseini, A. Darabi, and M. Assili, "Analytical and experimental analysis of back EMF waveform of a TORUS-type non-slotted axial flux permanent magnet synchronous machine with shifted rotor," *Meas. J. Int. Meas. Confed.*, vol. 156, 2020, doi: 10.1016/j.measurement.2020.107620.
- [31] J. Yang et al., "Design and analysis of a novel permanent magnet homopolar inductor machine with mechanical flux modulator for flywheel energy storage system," *IEEE Trans. Ind. Electron.*, vol. 69, no. 8, 2022, doi: 10.1109/TIE.2021.3104583.
- [32] Y. Cao and C. Liu, "Design and analysis of a dual-direction hybrid excitation generator," *IEEJ Trans. Electr. Electron. Eng.*, vol. 17, no. 11, 2022, doi: 10.1002/tee.23674.
- [33] M. Zhang, A. Bodrov, R. Shuttleworth, and M. F. Iacchetti, "Current-modulation-based on-line resonance tuning strategy for linear generator drives," *IEEE Trans. Ind. Electron.*, vol. 68, no. 4, 2021, doi: 10.1109/TIE.2020.2978697.
- [34] Y. Zhang, B. Yang, D. Ji, X. Hou, B. Zhao, and T. Zhang, "Integrated simulation and performance analysis of confined piston linear generator (CPLG)," *Energy*, vol. 282, 2023, doi: 10.1016/j.energy.2023.128814.
- [35] B. C. Kim and D. W. Kang, "A study on the novel design to improve efficiency of wound field synchronous machine," *IEEE Trans. Magn.*, vol. 57, no. 2, 2021, doi: 10.1109/TMAG.2020.3013260.
- [36] Agarala, S. S. Bhat, D. Zychma, and P. Sowa, "A novel approach to using dual-field excited synchronous generators as wind power generators," *Energies*, vol. 17, no. 2, 2024, doi: 10.3390/en17020456.
- [37] Y. Chen, Y. Wang, W. Li, and C. Qin, "Modeling and fault-tolerant control method of multiphase permanent magnet pulsed alternator," *IEEE Trans. Plasma Sci.*, vol. 52, no. 7, pp. 2917–2925, Jul. 2024, doi: 10.1109/TPS.2024.3443342.
- [38] Amany R. Nasr, Ebrahim A. Badran, and Ibrahim I. I. Mansy, "A novel cooling technique to improve the thermal characteristics of a permanent magnet generator using an earth–air heat exchanger," *J. Electr. Comput. Eng.*, vol. 2025, Art. ID 9987298, 20 pages, doi: 10.1155/jece/9987298.
- [39] C. Z. Liaw, W. L. Soong, and N. Ertugrul, "Low-speed output power improvement of an interior PM automotive alternator," in *Conf. Rec. IAS Annu. Meeting (IEEE Ind. Appl. Soc.)*, 2006. doi: 10.1109/IAS.2006.256516.